Histol Histopathol (2013) 28: 725-735
DOI: 10.14670/HH-28.725

http://www.hh.um.es

Histology and Histopathology
Cellular and Molecular Biology

Nrf1 is time-dependently expressed and distributed in the distinct cell types after trauma to skeletal muscles in rats

Shu-Tao Zhang[1,2], Rui Zhao[1], Wen-Xiang Ma[1], Yan-Yan Fan[1], Wen-Zheng Guan[1], Jiao Wang[3], Peng Ren[1], Kun Zhong[2], Tian-Shui Yu[1], Jing-Bo Pi[4] and Da-Wei Guan[1]

[1]Department of Forensic Pathology, China Medical University School of Forensic Medicine, Shenyang, China, [2]Institute of Forensic Science, Heilongjiang Public Security Department, [3]Department of Physiology, Harbin Medical University and [4]Division of Translational Biology, The Hamner Institutes for Health Sciences, Research Triangle Park, NC, USA

Summary. Our goal was to elucidate the dynamic expression and distribution of the nuclear factor erythroid-derived factor 2-related factor 1 (Nrf1) by immunohistochemistry, Western blotting, and real-time PCR during wound healing of contused skeletal muscle in rats. An animal model of skeletal muscle contusion was established in 40 Sprague-Dawley male healthy rats. Samples were taken at 6 h, 12 h, 1 day, 3 days, 5 days, 7 days, 10 days, and 14 days post-injury, respectively (5 rats in each posttraumatic interval). 5 rats were employed as control. A weak immunoreactivity of Nrf1 was observed in the sarcoplasm and nuclei of normal myofibers in control rats. Prominent immunostaining for Nrf1 was seen in a large number of polymorphonulcear cells, round-shaped mononuclear cells and spindle-shaped fibroblastic cells, and regenerated multinucleated myotubes in the injured tissue. Subsequently, neutrophils, macrophages and myofibroblasts were identified as expressing Nrf1 by double immuno-fluorescent procedures. By real-time PCR analysis, Nrf1 expression was up-regulated and peaked at inflammatory phase. The expression tendency was also confirmed by Western blot. In conclusion, Nrf1 is time-dependently expressed in certain cell types, such as neutrophils, macrophages, myofibroblasts and regenerated multinucleated myotubes, suggesting that Nrf1 may modulate oxidative stress response and regeneration after trauma to skeletal muscles.

Offprint requests to: Da-Wei Guan, M.D., Ph.D., Department of Forensic Pathology, China Medical University School of Forensic Medicine, No. 92, Beier Road, Heping District, Shenyang 110001, Liaoning Province, P.R. China. e-mail: dwguan@mail.cmu.edu.cn or dwguan007@yahoo.com.cn

Key words: Skeletal muscle, Trauma, Nrf1, Wound repair

Introduction

Skeletal muscle wound healing is a complex physiological process which consists of three overlapping phases, degeneration and inflammation, muscle regeneration, and fibrosis. The process is characterized by rupture and ensuing necrosis of the myofibers, polymorphonulcear cells (PMNs) and round-shaped mononuclear cells (MNCs) infiltration, and spindle-shaped fibroblastic cells (FBCs) proliferation (Filippin et al., 2009; Yu et al., 2010). The process depends upon a coordinated action of a series of factors such as cytokines, tumour necrosis factor (TNF), growth factors, and so on over time (Broughton et al., 2006a). During the inflammatory phase, infiltrating neutrophils and macrophages not only phagocytize cellular debris and accelerate muscle degeneration, but also have subsequent influence on muscle regeneration and the development of fibrosis by releasing a series of free radicals, cytokines and growth factors (Prisk and Huard, 2003). Several studies show that acute oxidative stress modulates inflammatory response and inhibits muscle wound healing after skeletal muscle contusion (Ghaly and Marsh, 2010a,b).

Nrf (nuclear factor erythroid-derived factor 2-related factor) 1, which is also known as NFE2L1/LCRF1/TCF11, belongs to the family of cap'n'collar (CNC) basic leucine zipper (Chan et al., 1993). Nrf1 is ubiquitously distributed in mammalian cells and plays important roles in the regulation of gene expression, tissue differentiation and development, anti-oxidative

stress and inflammatory response in a variety of organisms (Chan et al., 1998; Kwong et al., 1999; Myhrstad et al., 2001; Chen et al., 2003; Leung et al., 2003; Biswas and Chan, 2010). Nrf1 has two major isoforms, the long isoform (120-kDa) and the short isoform (65-kDa) (Wang et al., 2007). The 65-kDa isoform of Nrf1 is nuclear, and as an integral membrane protein, the 120-kDa isoform is localized primarily in the endocytoplasmic reticulum (ER) (Wang and Chan, 2006). Both isoforms have the potential to modulate antioxidative stress (Wang et al., 2007; Zhao et al., 2011). Since wound healing after skeletal muscle contusion is a typical inflammation-evoked event, we suppose that Nrf1 may be up-regulated at both gene and protein level in response to the trauma.

In the present study, we investigated cell types expressing Nrf1 and correlation between Nrf1 and the posttraumatic interval during skeletal muscle wound healing by immunofluorescent technique, Western blotting and real-time PCR using an established animal model.

Materials and methods

Animal model of skeletal muscle contusion

A total of 45 healthy, adult Sprague–Dawley (SD) male rats, weighing 280-320g, were used. Establishment of the standardized animal model of skeletal muscle contusion in rats has been described previously, which was controllable and reproducible using a self-designed mechanical weight-drop device (Yu et al., 2010). Because instant impact velocity (V) and elastic deformation (DF) at the time of impact are key parameters for impact intensity (Lighthall, 1988), V and DF were monitored and recorded during the experimentation, which makes the severity of the contusions identical as far as possible. Briefly, 40 rats were anesthetized by intraperitoneal injection with 2% sodium pentobarbital (30 mg/kg). Subsequently, the rats were placed on experimental table in a prone position, and a single impact at velocity of 3 m/s was delivered to the site of the right posterior limb 2.5 cm away from calcaneus with 7.5 mm for DF. The size of impact interface of the counterpoise (weighing 500 g) was 1.127 cm^2. The energy transmitted to the right posterior limb was calculated to be 2.25 J as calculated by the equation: $E=1/2mv^2$. After injury, each rat was housed individually and kept under a 12-h light–dark cycle and specific pathogen-free conditions with free access to commercial rat chow and tap water. The rats were killed by intraperitoneal injection of a lethal dose of pentobarbital (350 mg/kg) at 6 h, 12 h, 1 day, 3 days, 5 days, 7 days, 10 days and 14 days posttrauma (5 rats at each posttraumatic interval). Muscle sample was dissected from the wound site and equally divided into two parts in each rat. One part was used for immunohistochemical procedure, and another was immediately frozen in liquid nitrogen for Western blotting and real-time PCR, respectively. For the 5 control rats, specimens were harvested from the same site after anesthetization with an over-dose of pentobarbital. Experiments complied with the "Principles of Laboratory Animal Care" (National Institutes of Health published no 85-23, revised 1985) that sought to minimize both the number of animals used and any suffering that they might experience and were performed according to the Guidelines for the Care and Use of Laboratory Animals of China Medical University.

Tissue preparation and immunohistochemical staining

The skeletal muscle specimens were immediately fixed in 4% paraformaldehyde in phosphate-buffered saline (PBS) (pH 7.4). 5 μm-thick paraffin sections were prepared. Immunostaining for Nrf1 was performed by streptavidin–peroxidase method. After deparaffinization, sections were rehydrated with a series of graded alcohol, and then heated in 0.01 mol/L sodium citrate buffer (pH 6.0) with a medical microwave oven for antigen retrieval. Subsequently, 0.3% H_2O_2-PBS was applied to eliminate endogenous peroxidase. The sections were blocked with 10% non-immune goat serum to reduce non-specific reaction. Then, tissue sections were incubated with rabbit anti-Nrf1 polyclonal antibody (dilution 1:400; sc-13031, Santa Cruz Biotechnology, CA, USA) overnight at 4°C, followed by incubation with Histostain-Plus Kit according to the manufacturer's instructions (Zymed Laboratories, South San Francisco, CA, USA). As immunohistochemical controls, some sections were incubated with normal rabbit IgG or PBS in place of the primary antibody. Nuclei were counterstained with hematoxylin.

In addition, hematoxylin-eosin (H-E) staining was conventionally conducted.

Cellular localization of Nrf1

Detection of Nrf1 in neutrophils, macrophages or myofibroblasts was conducted by double indirect immunofluorescent procedure. Briefly, deparaffinized sections were blocked with 5% BSA and incubated with rabbit anti-Nrf1 polyclonal antibody (dilution 1:400; sc-13031, Santa Cruz Biotechnology, CA, USA). Thereafter, the sections were incubated with biotinylated donkey anti-rabbit IgG (dilution 1:200) and streptavidin, Alexa Fluor® 555 conjugate (dilution 1:400). Then, tissue sections were further incubated with mouse anti-myeloperoxidase (MPO) monoclonal antibody (dilution 1:50; sc-33596, Santa Cruz Biotechnology), or anti-Macrophage Marker (MAC387) monoclonal antibody (dilution 1:50; sc-66204, Santa Cruz Biotechnology), or anti-α-smooth muscle actin (α-SMA) monoclonal antibody (dilution 1:200; MS-113, Lab Vision Corporation, Fremont, CA, USA) overnight at 4°C. After incubation with Alexa Fluor® 488 donkey anti-mouse IgG (dilution 1:200; A21202, Invitrogen) at room temperature for 2 h, the sections were mounted and

observed under a fluorescence microscope. The immunofluorescent images were digitally merged.

For positive cell ratio evaluation, 10 microscopic fields were randomly selected at 400-fold magnification in the wound zones in each section, and the ratio of Nrf1-positive cells to the total number of cells in each positive cell type was calculated in each microscopic field. The average ratio of the 10 selected microscopic fields was evaluated in each wound specimen and expressed as percentage.

Protein preparation and immunoblotting assay

The skeletal muscle samples were diced into very small pieces using a clean razor blade and homogenized with a sonicator in RIPA buffer (sc-24948, Santa Cruz Biotechnology) containing protease inhibitors at 4°C. Homogenates were centrifuged at 12,000xg for 30 min at 4°C three times, and the resulting supernatants were collected. The protein concentrations were determined by BCA method. Aliquots of the supernatants were diluted in an equal volume of 5x electrophoresis sample buffer and boiled for 5 min. Protein lysates (50 μg) were separated on a 10% sodium dodecyl sulfate-polyacrylamide electrophoresis gel and transferred onto polyvinylidene fluoride membranes (Millipore, Billerica, MA, USA). After being blocked with 5% non-fat dry milk in Tris-buffered saline-Tween#20 at room temperature for 2 h, the blots were incubated with rabbit anti-Nrf1 polyclonal antibody (dilution 1:300; sc-13031, Santa Cruz Biotechnology) at 4°C overnight and horseradish peroxidase conjugated goat anti-rabbit IgG (sc-2004, Santa Cruz Biotechnology) at 1:5,000 dilution at room temperature for 2 h. The blotting was visualized with Western blotting luminol reagent (sc-2048, Santa Cruz Biotechnology) by Electrophoresis Gel Imaging Analysis System (MF-ChemiBIS 3.2, DNR Bio-Imaging Systems, ISR). Subsequently, densitometric analyses of the bands were semi-quantitatively conducted using Scion Image Software (Scion Corporation, MD, USA). The relative protein levels were calculated by comparison with the amount of GAPDH (#G13-61M, signalchem, Canada) as a loading control.

Total RNA extraction and real-time fluorescent quantitative PCR

The collection of total RNA has been described previously (Ma et al., 2011). OD values for each RNA sample were measured by ultraviolet spectrophotometer. A260/A280 ranged from 1.8 to 2.0. Then, the RNA was reversely transcribed into cDNA using PrimeScript™ RT reagent Kit (RR037A, Takara Biotechnology). The resulting cDNA was used for real-time PCR with the sequence-specific primer pairs for Nrf1 and GAPDH (Table 1). Real-time PCR amplification was performed by Applied Biosystems 7500 Real-Time PCR System using SYBR® PrimeScript™ RT-PCR Kit (RR081A, Takara Biotechnology). To exclude any potential contamination, negative controls were also performed with dH_2O instead of cDNA during each run. No amplification product was detected. The real-time PCR procedure was repeated at least three times for each sample.

Statistical analysis

Data were expressed as means±standard deviation. For Western blot or real-time PCR data, comparison was made between two groups and analyzed using SPSS for Windows 13.0. The one-way ANOVA was used for data analysis. Difference associated with $P<0.05$ was considered as statistically significant.

Results

Histological examination

In sections stained with hematoxylin and eosin, hemorrhage, edema, and degeneration were seen in the contused skeletal muscle. A few PMNs appeared at wound zones at 6 h, which remarkably increased in number at 12 h post-wounding. At 1 day and 3 days post-injury, a large number of MNCs accumulated in the wounds. At 3 days post-wounding, FBCs appeared in the wound zones. From 5 to 10 days post-injury, a large number of FBCs, concomitant with regenerated multinucleated myotubes were observed in the wounds. At 14 days post-injury, fibrotic lesion was prominent in the area of contusion (Fig. 1a-f).

Immunohistochemical and double indirect immunofluorescence analyses

In the control skeletal muscle specimens, a weak positive immunoreactivity for Nrf1 was detected in

Table 1. Real-time PCR primer sequences.

Gene	Gen Bank ID	Species	Primer	Position	Product size (bp)
Nrf1	NM_001108293	Rodent	Forward:5'-CGCAAGCGCAAGTTGGA-3' Reverse:5'-GGCCTTATCTCGCTGCAAGT-3'	1030-1046 1079-1098	69
GAPDH	NM_017008.3	Rodent	Forward:5'- GGCACAGTCAAGGCTGAGAATG-3' Reverse:5'-ATGGTGGTGAAGACGCCAGTA-3'	242-263 364-384	143

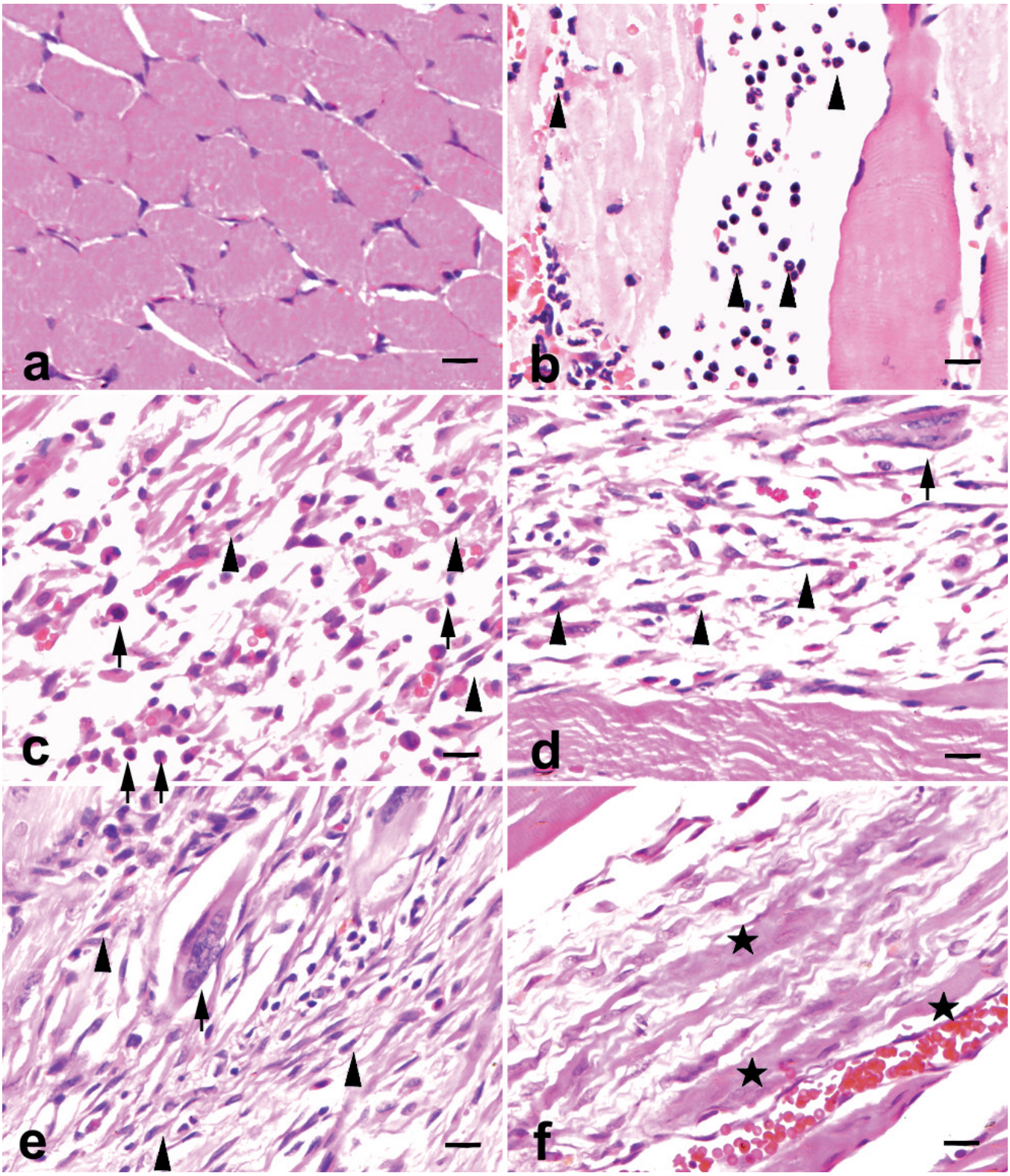

Fig. 1. Hematoxylin and eosin staining in rat skeletal muscle contusion. **a.** The morphology of normal sketetal muscle as a control. **b.** PMNs are detected at 12 h after injury (arrowheads). **c.** Round-shaped MNCs (arrows) and spindle-shaped FBCs (arrowheads) are present in the injured tissue at 3 days after injury. **d, e.** A large number of FBCs (arrowheads), concomitant with regenerated multinucleated myotubes (arrows) are observed in the area of contusion at 7 days **(d)** and 10 days **(e)** after injury. **f.** Fibrosis is prominent at 14 days post-wounding (asterisks). Scale bar: 10 μm

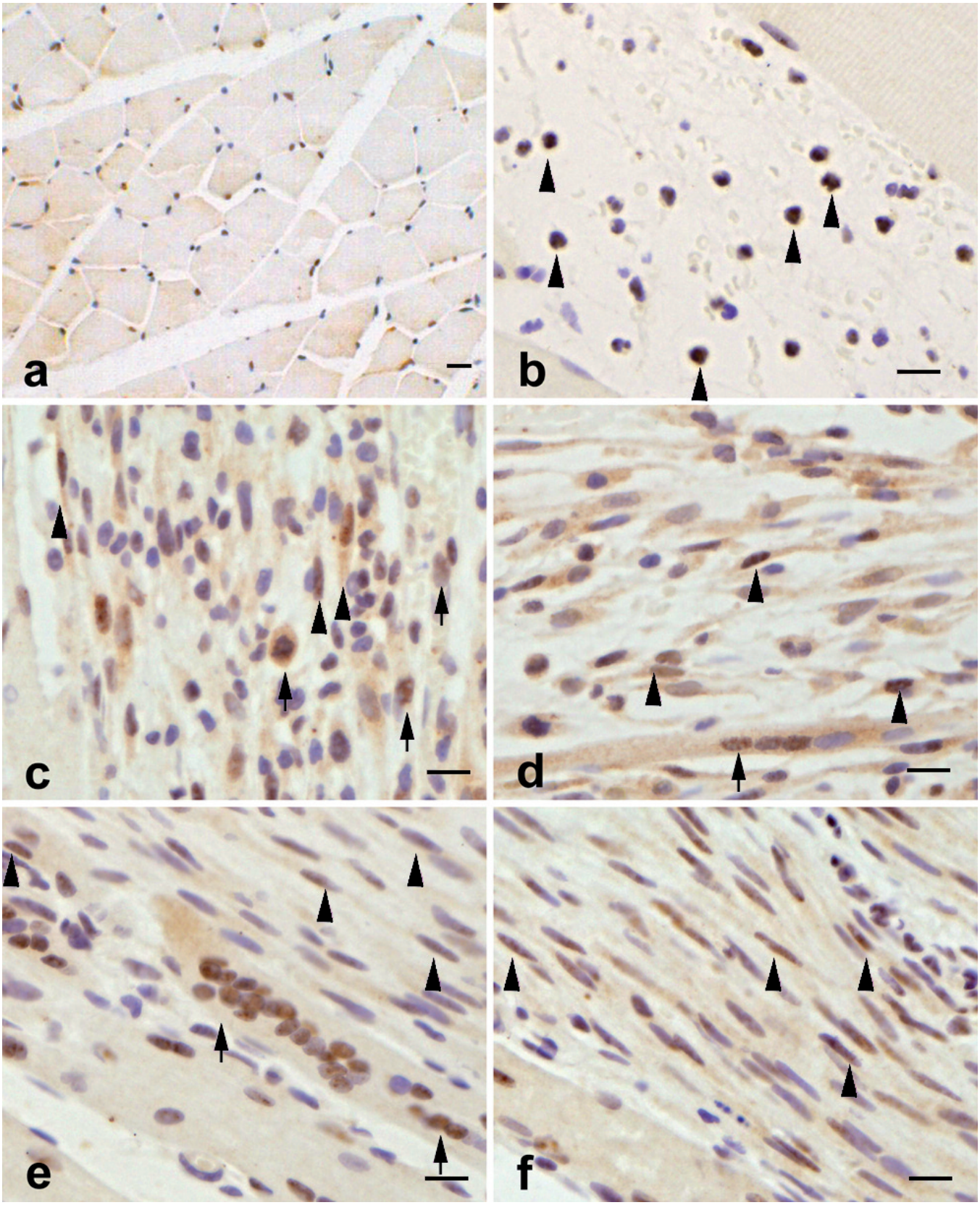

Fig. 2. Immunohistochemical staining of Nrf1 in rat skeletal muscle contusion. **a.** Nrf1 immunoreactivity is seen in sarcoplasm and nuclei of rat skeletal muscle. **b.** Nrf1-positive staining is observed in PMNs at 12 h after injury (arrowheads). **c.** At 3 days after injury, MNCs (arrows) and FBCs (arrowheads) reveal Nrf1-positive staining. **d, e.** A large number of FBCs (arrowheads) and regenerated multinucleated myotubes (arrows) are positively immunostained with antibody against Nrf1 in the wounded area at 7 days **d** and 10 days **e** post-injury. **f.** At 14 days post-wounding, there are a number of FBCs (arrowheads) labeled with anti-Nrf1 antibody in the fibrotic area. Scale bar: 10 μm

sarcoplasm and nuclei of rat skeletal muscle (Fig. 2a). In the injured skeletal muscle samples, a number of PMNs showed Nrf1-positive from 6 to 12h (Fig. 2b). At 1 and 3 days, a number of MNCs were positively immunostained with anti-Nrf1 antibody (Fig. 2c). From 5 to 10 days post-wounding, Nrf1 immunoreactivity was mainly detected in FBCs and regenerated multinucleated myotubes (Fig. 2d,e). At 14 days post-wounding, there were still a number of FBCs labeled with anti-Nrf1 antibody in fibrotic lesion (Fig. 2f). In addition, positive immunoreactivities for Nrf1 were observed in the injured skeletal muscle cells (Fig. 2b-f).

For identification of PMNs, co-localization of Nrf1 and MPO were conducted by double indirect immunofluorescent method. In the control, no $Nrf1^+$/ MPO^+ cells were observed. At 6 and 12 h post-injury, a great number of PMNs infiltrated into the injured site showed $Nrf1^+$/ MPO^+ (Fig. 3A). After 1 day post-injury, the number of double-positive cells was reduced at the wound zones. Most PMNs appeared Nrf1-positive in both cytoplasm and nuclei.

For identification of MNCs, co-localization of Nrf1 and MAC387 were conducted by double indirect immunofluorescent method. In the control, a few $Nrf1^+$/ $MAC387^+$ cells were observed in the perimysium and epimysium of normal skeletal muscle. At 1 day and 3 days post-injury, a large number of MNCs infiltrated into the injured site showed $Nrf1^+$/ $MAC387^+$ (Fig. 3B). From 7 days post-injury, fewer double-positive cells were detected at the wound zones. Most $MAC387^+$ cells were Nrf1-positive in both cytoplasm and nuclei and a few $MAC387^+$ cells Nrf1-negative.

For identification of FBCs, co-localization of Nrf1 and α-SMA were conducted by double indirect immunofluorescent method. At 3 days post-injury, a few Nrf1+/α-SMA + cells appeared in the wound sites. With extension of posttraumatic interval, a lot of $Nrf1^+$/α-SMA+ cells were noted and only a few α-SMA^+ cells were found Nrf1-positive in nuclei (Fig. 3C). After 10 days post-injury, $Nrf1^+$/α-SMA^+ cells decreased in number gradually.

In each Nrf1-positive cell type, there was significant difference between two adjacent posttraumatic intervals (Table 2). The average ratios of Nrf1-positive neutrophils, macrophages or myofibroblasts were

Table 2. The average ratios of Nrf1-positive neutrophils, macrophages or myofibroblasts in relation to wound age.

Group	*x±s* (neutrophils)	*x±s* (macrophages)	*x±s* (myofibroblasts)
control	0	7.82±1.28	0
6 h	52.63±3.82	38.99±4.21	0
12 h	31.99±2.51	45.21±3.98	0
1 d	12.11±1.89	59.13±3.79	0
3 d	8.21±1.54	46.85±4.97	9.32±1.83
5 d	6.58±1.13	41.23±2.35	31.67±2.28
7 d	5.53±1.12	36.78±2.27	51.36±4.35
10 d	0	35.23±2.96	39.28±2.25
14 d	0	31.57±3.26	32.45±4.13

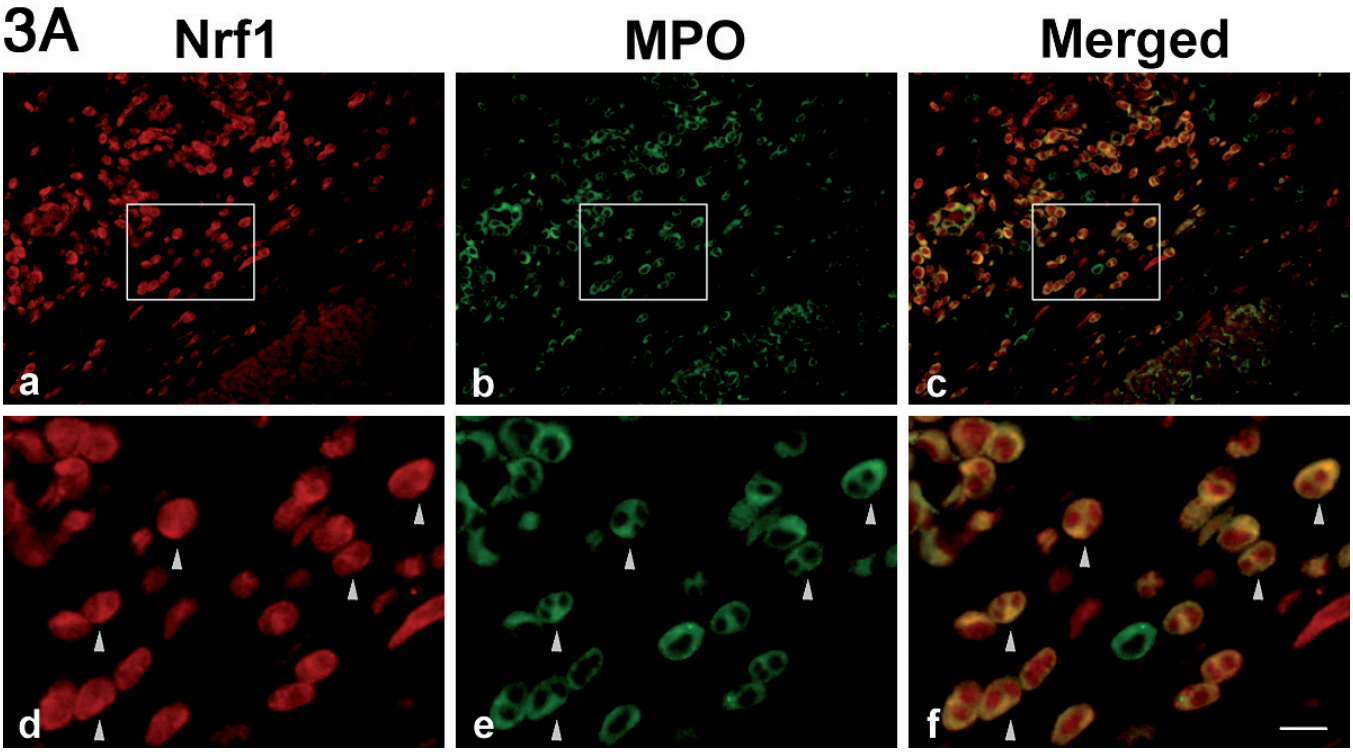

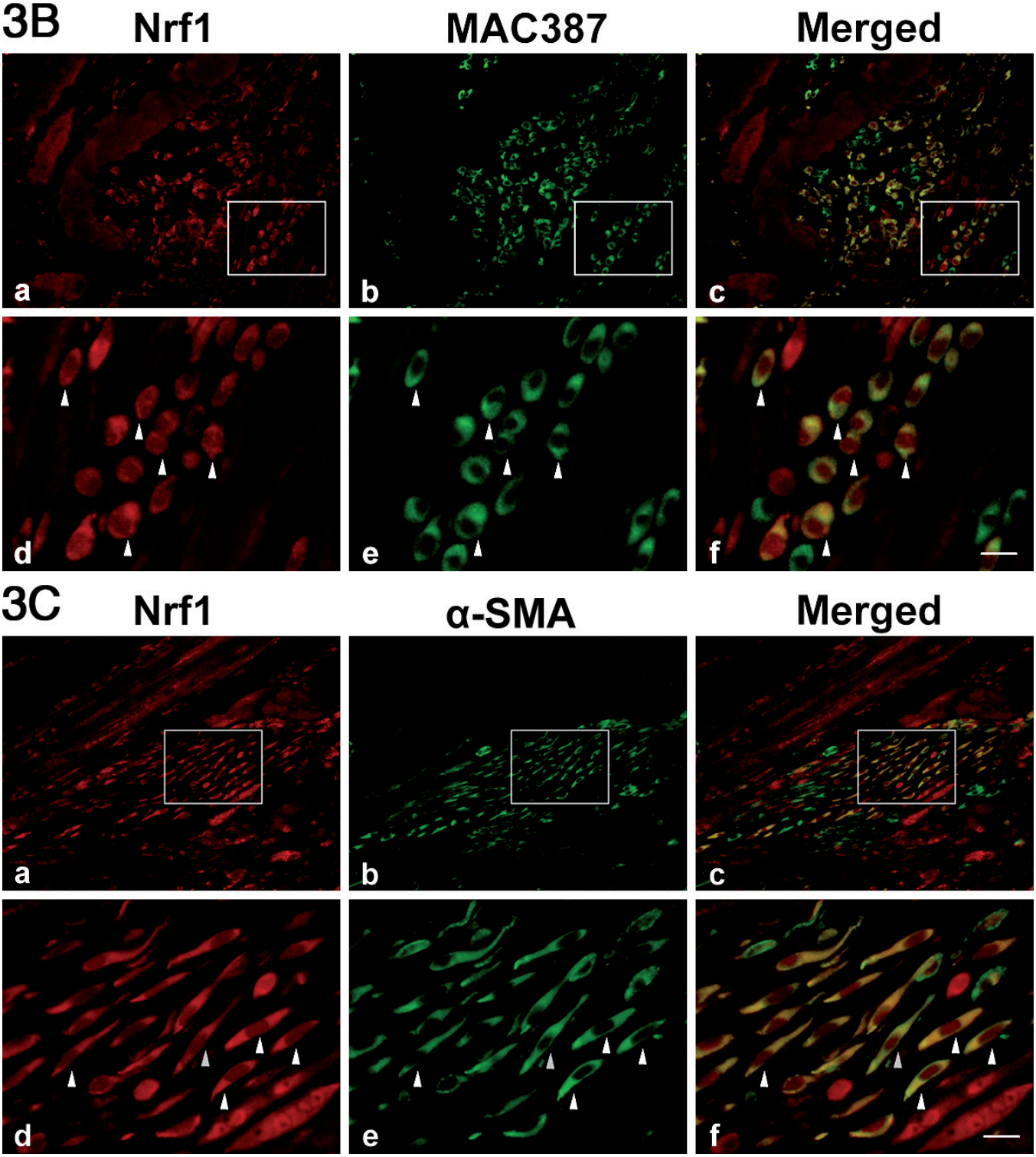

Fig. 3. A-C. Double immunofluorescent analysis for identification of the cell types expressing Nrf1 at 12 h **(A)**, 3 days **(B)** and 7days **(C)** post-injury (arrowheads). The samples are co-labeled with anti-Nrf1 **(A, B and C; red)** and anti-MPO **(A; green)**, anti-MAC387 **(B; green)**, or anti-α-SMA **(C; green)**. Signals in panel a and b are digitally merged in panel c under low magnification. Panels d, e and f are high magnification of panels a, b and c, respectively. Representative results from three independent experiments are shown here. Scale bar: 10 μm

evaluated (Fig. 4).

Western blotting and real-time fluorescent quantitative PCR

The blots against Nrf1 and GAPDH antibody are shown in Fig. 5a. Two bands were detected in the control and at each posttraumatic interval, which were located at 65 kDa and 120 kDa, respectively. The ratios of Nrf1 to GAPDH are shown in Table 3a-c. The average ratio of Nrf1 to GAPDH peaked at 1 day post-injury, which was 2.47±0.09. Significant differences in the relative expression levels of Nrf1 protein were found between control group and 6 h, 12 h, 1 day, 3 days, 7 days, 10 days, or 14 days posttraumatic groups. There were significant differences in the relative intensity of Nrf1 to GAPDH between 6 h, 12 h, 1 day or 3 days injury groups and their preceding groups (Fig. 5b). The relative intensity of P65Nrf1 or P120Nrf1 to GAPDH are shown in Fig. 5c,d.

Relative quantity of Nrf1 mRNA expression in rat skeletal muscle was assayed by real-time PCR throughout the 14 days after contusion. There were significant differences between control group and 6 h, 1 day, 3 days or 5 days post-injury in the expression of Nrf1 mRNA. Significant differences in the relative quantity of Nrf1 mRNA were found between 6 h, 12 h, 1 day, 3 days or 7 days injury groups and their preceding

Table 3a. The average ratios of Nrf1 to GAPDH in each group (n=5).

Group	*x±s*
control	2.07±0.08#*
6 h	2.45±0.08#*
12 h	2.26±0.10#*
1 d	2.47±0.09#*
3 d	2.20±0.05#*
5 d	2.12±0.04
7 d	2.21±0.06#
10 d	2.16±0.07#
14 d	2.22±0.05#

All values are expressed as the means±SEM (n=5). #P<0.05 (vs each posttraumatic group) *P<0.05 (vs preceding posttraumatic group).

Table 3b. The average ratios of P65Nrf1 to GAPDH in each group (n=5).

Group	*x±s*
control	0.93±0.04
6 h	1.34±0.03#*
12 h	1.11±0.05#*
1 d	1.32±0.05#*
3 d	1.26±0.14#
5 d	1.12±0.02#*
7 d	1.18±0.02#
10 d	1.11±0.03#
14 d	1.16±0.02#

All values are expressed as the means±SEM (n=5). #P<0.05 (vs each posttraumatic group) *P<0.05 (vs preceding posttraumatic group).

Table 3c. The average ratios of P120Nrf1 to GAPDH in each group (n=5).

Group	*x±s*
control	1.13±0.05
6 h	1.12±0.06
12 h	1.16±0.06
1 d	1.15±0.06
3 d	1.01±0.05#*
5 d	1.00±0.04#
7 d	1.02±0.05#
10 d	1.05±0.05#
14 d	1.05±0.05#

All values are expressed as the means±SEM (n=5). #P<0.05 (vs each posttraumatic group) *P<0.05 (vs preceding posttraumatic group).

Table 4. The average ratios of Nrf1 mRNA expression in each group (n=5).

Group	*x±s*
control	1.00±0.00
6 h	1.47±0.11#*
12 h	1.13±0.07*
1 d	2.09±0.10#*
3 d	1.70±0.08#*
5 d	1.65±0.07#
7 d	1.10±0.08*
10 d	0.94±0.05
14 d	1.05±0.12

All values are expressed as the means±SEM (n=5). #P<0.05 (vs each posttraumatic group) *P<0.05 (vs preceding posttraumatic group).

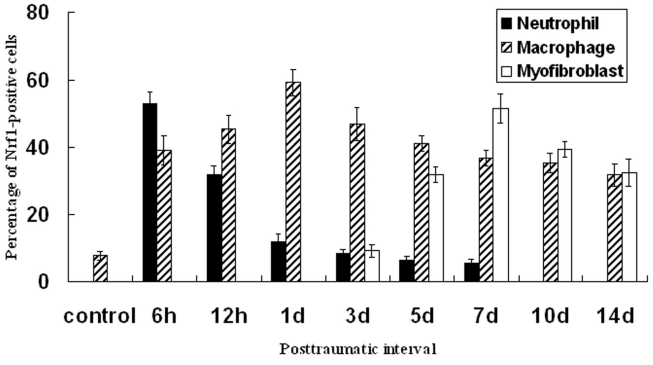

Fig. 4. The average ratios of Nrf1-positive neutrophils, macrophages and myofibroblasts in relation to wound age.

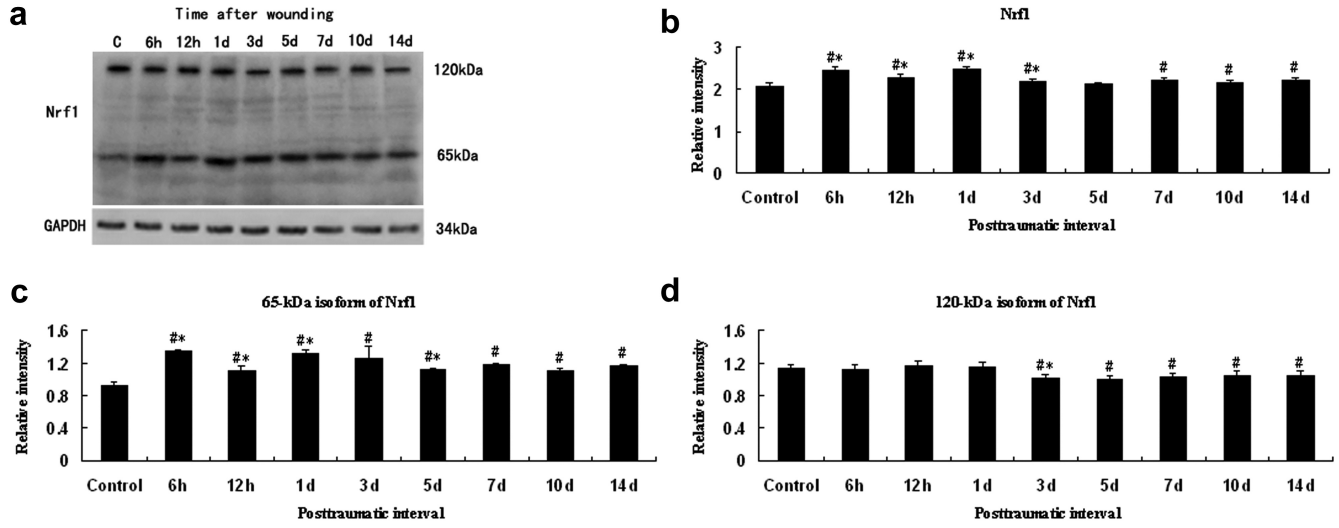

Fig 5. a. Analysis of Nrf1 and GAPDH protein from skeletal muscle specimens by Western blotting. Lane C represents the control skeletal muscle. Representative results from five individual animals are shown. **b.** Relative intensity of Nrf1 and GAPDH. **c.** Relative intensity of P65 Nrf1 and GAPDH. **d.** Relative intensity of P120Nrf1 and GAPDH. All values are expressed as the means ± SEM (n=5). #P<0.05 (vs each posttraumatic group); *P<0.05 (vs preceding posttraumatic group).

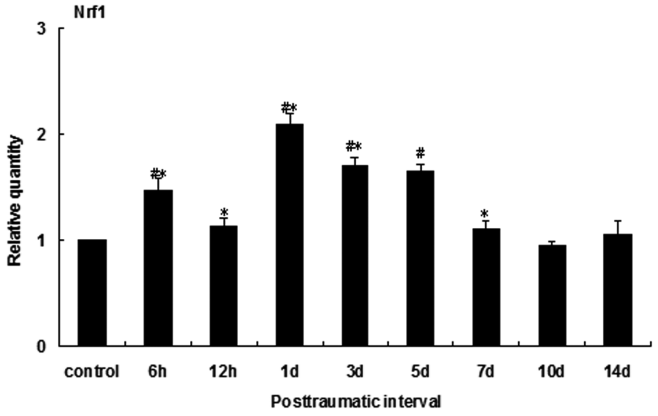

Fig. 6. Analysis of Nrf1 and GAPDH mRNA expression from skeletal muscle specimens by real-time PCR. #p<0.05 (vs each posttraumatic group); *p<0.05 (vs preceding posttraumatic group)

groups (Fig. 6).

Discussion

Wound healing is a complex series of reactions and interactions among cells and "mediators" and is generally divided into three phases: inflammatory, proliferation, and maturation (Broughton et al., 2006b). Damage to skeletal muscle due to blunt trauma presented pathologically a typical inflammatory process during repair. In the short term following impact (<24 h post-injury), the damaged segments show gross tearing and degeneration with numerous inflammatory cells infiltration (Fisher et al., 1990). 24 h after injury macrophages are the predominant cell type in injury zones (Papadimitriou et al., 1990). From 3 days post-injury onward, myotubes are present in the wound zones, and augmented remarkably at 7 days (Robertson et al., 1993). Our present study confirmed similar findings on morphological changes.

Recent researches show that oxidative stress may play an important part in the inflammatory processes after muscle injury and repair (Tidball, 2005; Ghaly and Marsh, 2010b). The mechanisms of inflammatory processes might include down-regulation of chemokine expression by anti-inflammatory cytokines or up-regulation of anti-inflammatory molecules (Eming et al., 2007). A potential mechanism by which inflammatory or other cells could induce skeletal muscle injury after acute trauma is through the generation of reactive metabolites of nitrogen and oxygen, which can cause additional damage to proteins, lipids and nucleic acids (Pizza et al., 1998). However, there are no definitive findings to show which factors are functionally important in manipulation of muscle injury and repair. Among the numerous factors, Nrf1 may play a role in modulating the inflammatory response (Suliman et al., 2010; van Tienen et al., 2010).

Nrf1 is widely distributed and abundantly present in tissues and organs (Biswas and Chan, 2010). After binding to the antioxidant response element (ARE), Nrf1 acts as a dominant factor to modulate antioxidative stress response by regulating the expression of GCS, together with other components of the pathway, and in this way

plays a role in regulating cellular glutathione levels. Glutathione (GSH) or gamma-glutamylcysteinylglycine executes important protective functions in the cells through elimination of xenobiotics and free radicals and maintenance of the intracellular redox balance (Myhrstad et al., 2001; Biswas and Chan, 2010). Nrf1 is shown to be involved in the transcriptional up-regulation of cytoprotective genes, including those encoding glutamate cysteine ligase, NAD(P)H:quinone oxidoreductase, glutathione S-transferases and aldo-keto reductases (Mathers et al., 2004). Fetal livers from Nrf1 mutant embryos enhance sensitivity to oxidative stress and impair expression of antioxidant genes (Chen et al., 2003). These data indicate that Nrf1 may play important roles in the regulation of gene expression, anti-oxidative stress and inflammatory response in a variety of organisms. For the role of Nrf1 in repair after trauma, it is presumed that Nrf1 regulates the expression of some antioxidant stress genes during skeletal muscle wound healing.

Nrf1 is essential for development. Nrf1 deficient function in mice leads to late gestational embryonic lethality. Mutant embryos suffer from anemia caused by abnormal fetal liver erythropoiesis that is non-cell autonomous. Although it has been suggested that Nrf1 plays a role in globin gene regulation, no defect in expression of globin genes is detected in erythrocytes (Chan et al., 1998). Fibroblasts derived from Nrf1 null embryos show decreased glutathione levels and are hypersensitive to the toxic effects of oxidant compounds (Kwong et al., 1999). In adult mouse liver, a specific inactivated Nrf1 gene can lead to steatohepatitis and hepatic neoplasia (Xu et al., 2005). Besides, Nrf1 also plays an important role in bone development as osteoblast-specific Nrf1 knockout mice have less bone mineral content and bone area (Biswas and Chan, 2010). In our study, Nrf1 was expressed in regenerated multinucleated myotubes, suggesting that Nrf1 may be involved in promoting skeletal muscle regeneration after wounding.

It has been experimentally shown that transforming growth factor-ß (TGF-ß) treatment of human smooth muscle cells leads to increased expression and binding of Nrf1/MafG heterodimers, suggesting that there is a novel mechanism by which iNOS expression is regulated in the context of inflammatory activation (Berg et al., 2007). Knockdown of Nrf1 blocks the suppression of iNOS expression by TGF-ß (Ohtsuji et al., 2008). In addition, a study has demonstrated that iNOS upregulation occurs in skeletal muscle fibers during inflammatory myopathies (Tews and Goebel, 1998). The generation of NO during the inflammatory response occurs mainly by the inducible isoform of NO synthase (iNOS), which plays a crucial role in numerous and diverse pathophysiological processes, including the healing of trauma to the skeletal muscle (Nathan and Hibss, 1991; Filippin et al., 2011). Therefore, Nrf1 may function during skeletal muscle wound healing and can perhaps act on the pathway of TGF-ß suppressing the expression of iNOS.

Myofibroblasts are the predominant proliferating cells during the proliferative phase (Broughton et al., 2006a). It has been found that fibroblasts derived from Nrf1 null embryos show decreased glutathione levels and are hypersensitive to the toxic effects of oxidant compounds (Kwong et al., 1999). In our study, we demonstrated that Nrf1 was widely expressed in neutrophils, macrophages and myofibroblasts, and Nrf1 was evidently up-regulated at protein and gene level from inflammatory phase to early proliferative phase after trauma to skeletal muscle. These findings suggested that wide expression of Nrf1 in neutrophils, macrophages and myofibroblasts might play a functional role in inflammation and wound repair via increased glutathione levels and reduced sensitivity to the toxic effects of oxidants during the healing process after skeletal muscle contusion.

Fibrosis is an inevitable result of mammalian wound repair. Abundant evidence shows that inflammation is an essential prerequisite for fibrosis and also regulates muscle regeneration and growth after muscle injury through the combined actions of free radicals, growth factors, and chemokines (Tidball, 2005; Broughton et al., 2006a; Eming et al., 2007). Macrophages can produce numerous cytokines and growth factors crucial for fibroblast recruitment and angiogenesis (Satish and Kathju, 2010). TGF-ß is believed to be responsible for fibrosis during skeletal muscle repair (Jarvinen et al., 2005). It has been indicated that NO is involved in the balance between fibrosis and healing with regeneration (Filippin et al., 2011). Up-regulation of Nrf1 suggests that Nrf1 may play a role in governing fibrotic events through activation of the TGF-ß pathway during repair of traumatized muscles.

In conclusion, up-regulation of expression and distribution of Nrf1 in distinct cell types suggests that Nrf1 is involved in modulating oxidative stress, fibrosis and skeletal muscle regeneration after trauma to skeletal muscles. Further investigation is needed for clarification of Nrf1 roles.

Acknowledgement. The study was financially supported in part by grants from research funds for the Doctoral Program funded by Ministry of Education of China (20122104110025) and National Natural Science Foundation of China (30271347).

W.Z. Guan is an undergraduate student of 7-year-program of Clinical Medicine of China Medical University.

References

Berg D.T., Gupta A., Richardson M.A., O'Brien L.A., Calnek D. and Grinnell B.W. (2007). Negative regulation of inducible nitric-oxide synthase expression mediated through transforming growth factor-beta-dependent modulation of transcription factor TCF11. J. Biol. Chem. 282, 36837-36844.

Biswas M. and Chan J.Y. (2010). Role of Nrf1 in antioxidant response element-mediated gene expression and beyond. Toxicol. Appl.

Pharmacol. 244, 16-20.

Broughton G.N., Janis J.E. and Attinger C.E. (2006a). The basic science of wound healing. Plast. Reconstr. Surg. 117, 12S-34S.

Broughton G.N., Janis J.E. and Attinger C.E. (2006b). Wound healing: an overview. Plast. Reconstr. Surg. 117, 1e-32e.

Chan J.Y., Han X.L. and Kan Y.W. (1993). Cloning of Nrf1, an NF-E2-related transcription factor, by genetic selection in yeast. Proc. Natl. Acad. Sci. USA 90, 11371-11375.

Chan J.Y., Kwong M., Lu R., Chang J., Wang B., Yen T.S. and Kan Y.W. (1998). Targeted disruption of the ubiquitous CNC-bZIP transcription factor, Nrf-1, results in anemia and embryonic lethality in mice. EMBO J. 17, 1779-1787.

Chen L., Kwong M., Lu R., Ginzinger D., Lee C., Leung L. and Chan J.Y. (2003). Nrf1 is critical for redox balance and survival of liver cells during development. Mol. Cell. Biol. 23, 4673-4686.

Eming S.A., Krieg T. and Davidson J.M. (2007). Inflammation in wound repair: molecular and cellular mechanisms. J. Invest. Dermatol. 127, 514-525.

Filippin L.I., Moreira A.J., Marroni N.P. and Xavier R.M. (2009). Nitric oxide and repair of skeletal muscle injury. Nitric Oxide 21, 157-163.

Filippin L.I., Cuevas M.J., Lima E., Marroni N.P., Gonzalez-Gallego J., and Xavier R.M. (2011). The role of nitric oxide during healing of trauma to the skeletal muscle. Inflamm. Res. 60, 347-356.

Fisher B.D., Baracos V.E., Shnitka T.K., Mendryk S.W. and Reid D.C. (1990). Ultrastructural events following acute muscle trauma. Med. Sci. Sports Exerc. 22, 185-193.

Ghaly A. and Marsh D.R. (2010a). Ischaemia-reperfusion modulates inflammation and fibrosis of skeletal muscle after contusion injury. Int. J. Exp. Pathol. 91, 244-255.

Ghaly A. and Marsh D.R. (2010b). Aging-associated oxidative stress modulates the acute inflammatory response in skeletal muscle after contusion injury. Exp. Gerontol. 45, 381-388.

Jarvinen T.A., Jarvinen T.L., Kaariainen M., Kalimo H. and Jarvinen M. (2005). Muscle injuries: biology and treatment. Am. J. Sports Med. 33, 745–764.

Kwong M., Kan Y.W. and Chan J.Y. (1999). The CNC basic leucine zipper factor, Nrf1, is essential for cell survival in response to oxidative stress-inducing agents. Role for Nrf1 in gamma-gcs(l) and gss expression in mouse fibroblasts. J. Biol. Chem. 274, 37491-37498.

Leung L., Kwong M., Hou S., Lee C. and Chan J.Y. (2003). Deficiency of the Nrf1 and Nrf2 transcription factors results in early embryonic lethality and severe oxidative stress. J. Biol. Chem. 278, 48021-48029.

Lighthall J.W. (1988). Controlled cortical impact: a new experimental brain injury model. J. Neurotrauma. 5, 1-15.

Mathers J., Fraser J.A., McMahon M., Saunders R.D., Hayes J.D., McLellan L.I. (2004). Antioxidant and cytoprotective responses to redox stress. Biochem. Soc. Symp. 71, 157-76.

Ma W.X., Yu T.S., Fan Y.Y., Zhang S.T., Ren P., Wang S.B., Zhao R., Pi J.B. and Guan D.W. (2011). Time-dependent expression and distribution of monoacylglycerol lipase during the skin-incised wound healing in mice. Int. J. Legal Med. 125, 549-558.

Myhrstad M.C., Husberg C., Murphy P., Nordstrom O., Blomhoff R., Moskaug J.O. and Kolsto A.B. (2001). TCF11/Nrf1 overexpression increases the intracellular glutathione level and can transactivate the gamma-glutamylcysteine synthetase (GCS) heavy subunit promoter. Biochim. Biophys. Acta 1517, 212-219.

Nathan C.F. and Hibbs J.B. Jr (1991). Role of nitric oxide synthesis in macrophage antimicrobial activity. Curr. Opin. Immunol. 3, 65-70.

Ohtsuji M., Katsuoka F., Kobayashi A., Aburatani H., Hayes J.D. and Yamamoto M. (2008). Nrf1 and Nrf2 play distinct roles in activation of antioxidant response elementdependent genes. J. Biol. Chem. 283, 33554-33562.

Papadimitriou J.M., Robertson T.A., Mitchell C.A. and Grounds M.D. (1990). The process of new plasmalemma formation in focally injured skeletal muscle fibers. J. Struct. Biol. 103, 124-134.

Pizza F.X., Hernandez I.J. and Tidball J.G. (1998). Nitric oxide synthase inhibition reduces muscle inflammation and necrosis in modified muscle use. J. Leukoc. Biol. 64, 427-33.

Prisk V. and Huard J. (2003). Muscle injuries and repair: the role of prostaglandins and inflammation. Histol. Histopathol. 18, 1243-1256.

Robertson T.A., Maley M.A., Grounds M.D. and Papadimitriou J.M. (1993). The role of macrophages in skeletal muscle regeneration with particular reference to chemotaxis. Exp. Cell Res. 207, 321-331.

Satish L. and Kathju S. (2010). Cellular and molecular characteristics of scarless versus fibrotic wound healing. Dermatol. Res. Pract. 2010, 790234.

Suliman H.B., Sweeney T.E., Withers C.M. and Piantadosi C.A. (2010). Co-regulation of nuclear respiratory factor-1 by NFkappaB and CREB links LPS-induced inflammation to mitochondrial biogenesis. J. Cell. Sci. 123, 2565-2575.

Tews D.S. and Goebel H.H. (1998). Cell death and oxidative damage ininflammatory myopathies. Clin. Immunol. Immunopathol. 87, 240–247.

Tidball J.G. (2005). Inflammatory processes in muscle injury and repair. Am. J. Physiol. Regul. Integr. Comp. Physiol. 288, R345-R353.

van Tienen F.H., Lindsey P.J., van der Kallen C.J. and Smeets H.J. (2010). Prolonged Nrf1 overexpression triggers adipocyte inflammation and insulin resistance. J. Cell. Biochem. 111, 1575-1585.

Wang W. and Chan J.Y. (2006). Nrf1 is targeted to the endoplasmic reticulum membrane by an N-terminal transmembrane domain. Inhibition of nuclear translocation and transacting function. J. Biol. Chem. 281, 19676-19687.

Wang W., Kwok A.M. and Chan J.Y. (2007). The p65 isoform of Nrf1 is a dominant negative inhibitor of ARE-mediated transcription. J. Biol. Chem. 282, 24670-24678.

Xu Z., Chen L., Leung L., Yen T.S., Lee C., Chan J.Y. (2005). Liver-specific inactivation of the Nrf1 gene in adult mouse leads to nonalcoholic steatohepatitis and hepatic neoplasia. Proc. Natl. Acad. Sci. USA 102, 4120–4125.

Yu T.S., Cheng Z.H., Li L.Q., Zhao R., Fan Y.Y., Du Y, Ma W.X. and Guan D.W. (2010). The cannabinoid receptor type 2 is time-dependently expressed during skeletal muscle wound healing in rats. Int. J. Legal Med. 124, 397-404.

Zhao R., Hou Y., Xue P., Woods C.G., Fu J., Feng B., Guan D., Sun G., Chan J.Y., Waalkes M.P., Andersen M.E. and Pi J. (2011). Long isoforms of NRF1 contribute to arsenic-induced antioxidant response in human keratinocytes. Environ. Health. Perspect. 119, 56-62.

Accepted October 29, 2012